J Prosthodont Res. 2023; **(**): ****–****

OPEN ACCESS JPR Journal of Prosthodontic Research Original article

Effect of abutment tooth location on the accuracy of digital impressions obtained using an intraoral scanner for removable partial dentures

Kazuki Sakamoto [a], Junichiro Wada [a,b,*], Yuki Arai [a,c], Hironari Hayama [a], Yurika Ishioka [a], Eung-Yeol Kim [a], Ryunosuke Kazama [a], Yusuke Toyoshima [a], Noriyuki Wakabayashi [a]

[a] Department of Advanced Prosthodontics, Graduate School, Tokyo Medical and Dental University (TMDU), Tokyo, Japan, [b] Department of Biomaterials Science and Turku Clinical Biomaterials Center – TCBC, Institute of Dentistry, University of Turku, Turku, Finland, [c] Department of Orthodontics, University of Texas Health Science Center at Houston School of Dentistry, Houston, TX, United States

Abstract

Purpose: To verify the effect of abutment tooth location on the accuracy of digital impressions obtained using an intraoral scanner (IOS) for removable partial dentures (RPDs).

Methods: The target abutment teeth included the left first premolar (#34), second molar (#37), and right second premolar (#45) in a mandibular Kennedy class II model and the left and right second molars (#37, #47) in a class III model. Only #37 was isolated from the remaining teeth by the mucosal area in both models. Digital impressions were obtained using a desktop scanner (reference data) and an IOS (IOS data; scanning origin #37; n=10). The general trueness based on the entire model superimposition (T_G), local trueness (T_L) of an individual tooth, and dimensional accuracy (coordinate and linear accuracy) of the IOS data of the target abutment teeth were compared (α=0.05).

Results: In both models, #37 showed significantly inferior T_G (P<0.01), superior T_L (P<0.01), and mesial coordinate displacement (P<0.01 and P<0.05 in class II and III models, respectively). Intra-model comparisons showed that #45 in the class II model and #47 in the class III model had significantly inferior linear accuracy (P<0.05 and P<0.01, respectively) and buccal coordinate displacement (P<0.05 and P<0.01, respectively) compared with the other target teeth.

Conclusions: In digital impressions of RPDs, isolation of abutment teeth by mucosal areas can reduce general trueness based on the entire dental arch and mesial tooth displacement, whereas increased distance from the scanning origin can adversely affect local trueness and dimensional accuracy.

Keywords: Accuracy, Digital impression, Intraoral scanner, Removable partial denture, Trueness

Received 26 July 2022, Accepted 4 November 2022, Available online 11 February 2023

1. Introduction

The use of digital technology in prosthetic treatment has been increasing recently, and digital impressions obtained using an intraoral scanner (IOS) have been clinically used in fixed prosthetic treatments such as dental implants[1], crown-bridges[2], and denture treatment[3]. Despite the various reported advantages of digital impressions, the application of digital impressions obtained by an IOS has been limited to removable partial denture (RPD) treatment. For Kennedy class III and IV dental arches with short-span mucosal areas, fabrication of RPDs using digital impression with an IOS has been recommended[4,5]. However, no studies have reported RPD fabrication using only a digital impression with an IOS for Kennedy class I and II dental arches with long-span mucosal areas and/or modified spaces.

Studies focusing on partially edentulous dental arches evaluated trueness and precision as measures of the accuracy of digital impression data obtained using an IOS[6,7]. According to the International Organization for Standardization, trueness is defined as the measured distance between the reference and target objects, and precision indicates the variability between repeated measurements during the impression process (ISO5725-1)[8]. A previous study reported that digital impressions obtained using an IOS showed superior trueness and inferior precision compared with those of conventional impressions prepared using elastic impression materials in mandibular Kennedy class I and III models[6]. Further studies reported that the trueness of the digital impression of a mandibular Kennedy class I model using an IOS was within the range of soft tissue displacement[7]. In addition, a modified space may lower the precision of the digital impression of the whole dental arch, including mucosal areas, in maxillary Kennedy class III and IV arches[9].

In partially edentulous dental arches with multiple mucosal areas, RPD abutment teeth adjacent to the mucosal areas are widely distributed in dentition. However, no previous report has presented a detailed evaluation of data accuracy based on individual RPD abut-

DOI: https://doi.org/10.2186/jpr.JPR_D_22_00201
***Corresponding author:** Junichiro Wada, Advanced Prosthodontics, Graduate School, Tokyo Medical and Dental University (TMDU), 1-5-45 Yushima, Bunkyo-ku, Tokyo 113-8549, Japan.
E-mail address: wadajun.rpro@tmd.ac.jp

ment tooth locations in digital impressions obtained using an IOS. To promote the clinical application of digital impressions in RPD treatment for partially edentulous patients with various defect types, the effect of abutment tooth location on the accuracy of digital impressions must be elucidated.

In this study, we evaluated the accuracy of digital impression data obtained using an IOS based on individual RPD abutment teeth located in various regions of the mandibular Kennedy class II model with a modified space and class III model. The purpose of this study was to verify the effect of RPD abutment tooth location on the accuracy of digital impression data for RPDs.

2. Materials and Methods

2.1. Digital data obtained using a high-accuracy desktop scanner (reference data)

Two types of partially edentulous mandibular dental arch models were used as reference models: a Kennedy class II, modification 1 model (E50-528; Nissin, Tokyo, Japan) with four missing teeth (left second premolar [#35] and first molar [#36] and the right first and second molars [#46 and #47]), three target RPD abutment teeth (the left first premolar [#34] and second molar [#37] and right second premolar [#45]); and a Kennedy class III model (E50-516; Nissin, Tokyo, Japan) with two missing teeth (the left second premolar [#35] and first molar [#36]) and two RPD abutment teeth (the left and right second molars [#37 and #47]). Among the target teeth of the class III model, only #37 was adjacent to the mucosal area and isolated from the remaining teeth. In the reference models, the artificial teeth, including the target teeth, were made of melamine resin, and the residual ridge was made of epoxy resin. To measure the digital impression data accuracy, we evaluated the trueness, deviation of the coordinate located on the abutment tooth (coordinate accuracy), and deviation in the distance from the lingual frenum (linear accuracy).

The reference data, which were used to evaluate the accuracy of the digital impressions obtained using an IOS, were obtained by scanning the reference models with a high-accuracy desktop scanner (ATOS TripleScan 16M; GOM, Braunschweig, Germany) (n = 1). This scanner exhibits a trueness of 3 µm for the jaw size[10]. The reference data were converted to standard triangulated language (STL) files and trimmed at the gingivobuccal fold and deepest lingual point using 3D modeling software (Geomagic Studio 2014; 3D Systems, Rock Hill, SC, USA). Errors caused by trimming in the preliminary experiment were examined, and their average value was 1.1 µm (n = 10).

2.2. Digital data acquisition using an IOS (IOS data)

Digital impression data for the reference models were obtained by full-arch scanning using an IOS (TRIOS3; 3Shape, Copenhagen, Denmark). All scans were performed by a single experienced operator (K.S.). In accordance with a previous study, the scans were initiated from the left side (#37) toward the right side over the occlusal surfaces of posterior teeth with straight motion and the incisal edges of anterior teeth with zigzag motion, followed by the lingual and then the buccal surfaces (**Fig. 1**)[11]. The full-arch scanned data were trimmed in the same manner as the reference data and converted to STL files as IOS data (n = 10 per model).

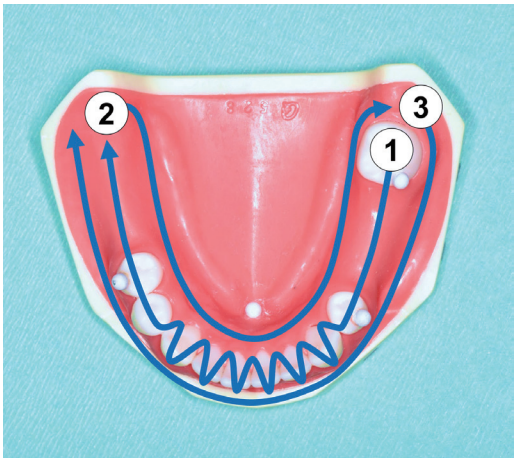

Fig. 1. Routine process for full-arch intraoral scanning of a mandibular partially edentulous arch model. The scanning begins with route (1) on the occlusal area with zigzag motions at the anterior teeth, followed by route (2) on the lingual surface, and then route (3) on the buccal surface.

2.3. Evaluation of trueness

The root mean square (RMS) value (µm) of the deviation at each STL structural point was calculated based on the reference data to represent the trueness of the IOS data. Using 3D analysis software (Geomagic Control X; 3D Systems, Rock Hill, SC, USA), the IOS data of the entire model were superimposed on the reference data using the best-fit method[12]. A line perpendicular to the facing surface at each STL structural point of the superimposed IOS data was then drawn to the surface of the reference data. The deviation (µm) between the STL structural point of the superimposed IOS data and the point of intersection of the perpendicular line and the surface of the reference data was calculated. The positive and negative values of the deviation indicated that the superimposed IOS data were positioned in the external and internal ranges of the reference data, respectively. The RMS values of deviations in all STL structural points in only the individual target abutment tooth area of the superimposed IOS data were calculated as the values representing the general trueness based on the entire model superimposition (T_G) for each target abutment tooth (**Fig. 2**). A higher RMS value indicated inferior trueness.

In addition, both the reference and IOS data were trimmed for each abutment tooth area, followed by data superimposition using the best-fit method. Subsequently, the RMS values of the deviations in all STL structural points were calculated as the value representing the local trueness based on individual abutment tooth superimposition (T_L) for each target abutment tooth.

2.4. Evaluation of coordinate accuracy and linear accuracy

To evaluate the accuracy of the dimensionality of the IOS data, the coordinates of the representative points on each target abutment tooth were measured using the lingual frenum as the reference point, and the three-dimensional differences in the coordinates of the IOS data relative to the reference data were calculated. Additionally, the distance (µm) from the lingual frenum was measured for each target tooth.

Stainless steel spherules with a diameter of 3 mm were placed on the buccal cusp of each target tooth (the mesial buccal cusp for

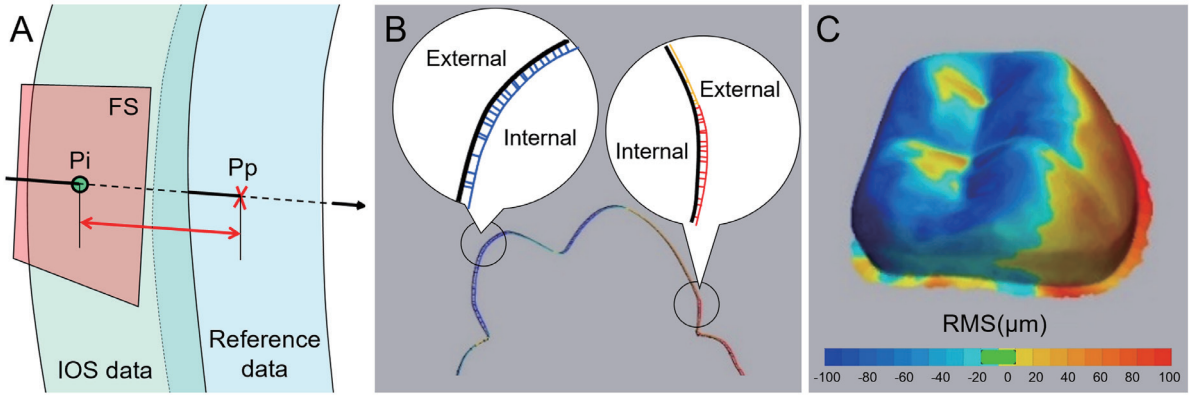

Fig. 2. Evaluation of trueness and representative color map images by deviation analyses performed using the best-fit method. A: After superimposition with the best-fit method, the perpendicular line (black arrow) of the facing surface (FS) at the STL structural point on the intraoral scanners (IOS) data (Pi) is drawn on the surface of the reference data. The distance between Pi and the point at the intersection of the perpendicular line and surface of the reference data (Pp) is calculated as the deviation (red arrow). B: Cross-sectional image of the individual target tooth (black and colored lines represent the reference data and superimposed IOS data, respectively). The color bar indicates the displacement (deviation) relative to the reference data. Positive scales represent the external position (yellow to red), whereas negative scales represent the internal position relative to the reference (light green to blue). The root-mean-square (RMS) value of the deviation represents trueness (the length of each line connecting the black and colored lines in (B)). C: Color map image of individual target abutment tooth analysis.

molars) and the lingual frenum. Reference data (n = 1) and IOS data (n = 10) were obtained in the same manner as described in Sections 2.1 and 2.2 for each reference model. To match the coordinate axes of the reference and IOS data, the IOS data were superimposed on the reference data using the best-fit method, followed by placement of the reference point on the center of the spherule on the lingual frenum in both the reference and IOS data (**Fig. 3A**). In both datasets, the coordinate axes were set as follows: the x-axis was parallel to both the basal and posterior surfaces of the reference data; the y-axis was perpendicular to the posterior surface of the reference data; and the z-axis was perpendicular to the basal surface of the reference data (**Fig. 3B**). Subsequently, the deviation of the center coordinate of the spherule on each abutment in the IOS data relative to the reference data was calculated to separately assess the coordinate accuracy along the x-, y-, and z-axes. The positive and negative values of the coordinate deviation indicated that the spherules on the superimposed IOS data were positioned in the following ranges of those on the reference data: left and right of the x-axis, distal and mesial of the y-axis, and above and below the z-axis. Additionally, a higher absolute value of the coordinate deviation indicated an inferior coordinate accuracy.

In addition, the distance between the central coordinate of the stainless steel spherule placed on each target tooth and that on the lingual frenum was measured (**Figs. 3C and D**). The rate of deviation in the distance in the IOS data relative to the reference data was calculated as a percentage, using the following equation:

$$R_d = [(D_I - D_R) / D_R] \times 100,$$

where R_d is the rate of deviation in distance (%), D_I is the distance in the IOS data in millimeters (mm), and D_R is the distance in the reference data in millimeters (mm). The positive and negative values of the rate of deviation indicated that the distance between the lingual frenum and each abutment tooth in the superimposed IOS data was greater and less than those in the reference data, respectively. The absolute value of the rate of deviation (%) was then calculated as the linear accuracy to compare the target teeth. A higher absolute value of the rate of deviation indicated inferior linear accuracy.

2.5. Statistical analysis

For each reference model, trueness (T_G and T_L), coordinate deviation, and linear accuracy were statistically compared among the target teeth. Because Levene's test did not confirm the homoscedasticity of the data, nonparametric tests were used. For the Kennedy class II model, the Friedman test was performed to detect any significant differences among the three target abutment teeth, followed by a *post-hoc* test for multiple comparisons if significant differences were found. For the class III model, the Wilcoxon signed-rank test was used to compare two target abutment teeth. In addition, the right second premolar in the class II model and the right second molar in the class III model were compared using the Mann–Whitney U test. The Bonferroni method was used to correct the p-values for multiple comparisons. SPSS predictive analytics software (version 24.0, SPSS Japan Inc., Tokyo, Japan) was used for the statistical analysis, and the significance level was set at $P<0.05$.

3. Results

3.1. Comparison of trueness

Figure 4 shows the general trueness based on the entire model superimposition (T_G) for both Kennedy class II and III models. In the class II model, the median (interquartile range [IQR]) T_G at #45, #34, and #37 were 42.3 (8.3) μm, 42.3 (12.2) μm, and 69.8 (19.2) μm, respectively. The T_G level at #37 was significantly higher than that at #34 ($P = 0.001$) and #45 ($P = 0.005$). In the class III model, the median (IQR) T_G at #47 and #37 was 48.5 (5.8) μm and 81.0 (42.6) μm, respectively. The T_G level at #37 was significantly higher than that at #47 ($P = 0.028$).

Figure 5 shows the local trueness based on the individual abutment tooth superimposition (T_L) for both the Kennedy class II and III models. In the class II model, the median (IQR) T_L at #45, #34, and #37 was 21.4 (3.0) μm, 21.4 (2.2) μm, and 15.1 (2.9) μm, respectively. The T_L at #37 was significantly lower than that at #45 ($P = 0.005$) and #34

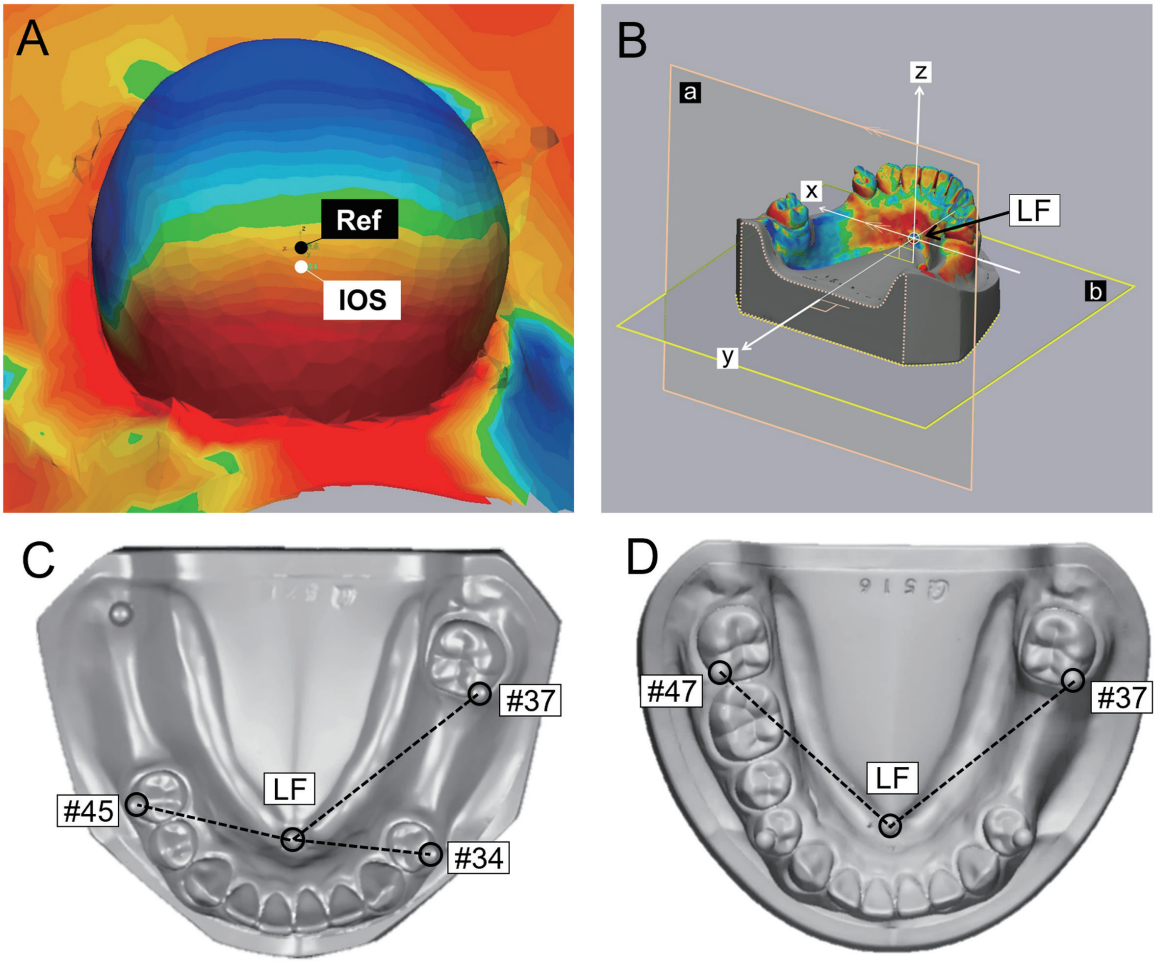

Fig. 3. Coordinate axes for the evaluation of coordinate accuracy and linear accuracy and the distance measured for comparisons of linear accuracy. A: After superimposition with the best-fit method, the center coordinate of the spherule placed on the lingual frenum (LF) was determined as the original point on each datum (the black and white points are the original points in the reference and intraoral scanners [IOS] data, respectively). B: The coordinate axes were set according to the following determinations: the x-axis was parallel to both the basal and posterior surfaces of the reference data, the y-axis was perpendicular to the posterior surface of the reference data, and the z-axis was perpendicular to the basal surface of the reference data. C: Distance used for linear accuracy comparison in the Kennedy class II model. D: Distance used for linear accuracy comparison in the Kennedy class III model.

($P = 0.004$). In the class III model, the median (IQR) T_L at #47 and #37 was 28.7 (3.9) μm and 23.6 (0.9) μm, respectively. The T_L at #47 was significantly higher than that at #37 ($P = 0.005$).

3.2. Comparison of coordinate accuracy

Table 1 presents the coordinate deviation in both Kennedy class II and III models. In the class II model, the Freidman test detected statistical significance among the three target abutment teeth along the x- and y-coordinates ($P = 0.001$ and $P < 0.001$, respectively). Multiple comparisons revealed that the coordinate deviation along the x-axis at #45 was significantly lower than that at #34 ($P = 0.001$) and #37 ($P = 0.042$), and that the coordinate deviation along the y-axis at #34 was significantly higher than that at #45 ($P = 0.042$) and #37 ($P < 0.001$). In the class III model, the Wilcoxon signed-rank test revealed that the coordinate deviation along the x-axis at #47 was significantly lower than that at #37 ($P = 0.005$) and that the coordinate deviation along the y-axis at #37 was significantly lower than that at #47 ($P = 0.047$).

3.3. Comparison of linear accuracy

Figure 6 shows the rate of deviation in the distance from the lingual frenum in both the Kennedy class II and III models. In the class II model, the median (IQR) rate of deviation and the real value of the difference in the distance at #45, #34, and #37 were 0.33% (0.15%) and 90.1 (41.8) μm, 0.07% (0.11%) and 18.3 (27.0) μm, and -0.11% (0.14%) and -40.9 (54.5) μm, respectively. In the class III model, the median (IQR) rate of deviation and the real value of the difference in the distance at #47 and #37 were 0.35% (0.08%) and 131.2 (30.7) μm and -0.10% (0.21%) and -37.8 (80.1) μm, respectively.

Figure 7 presents the linear accuracy in both Kennedy class II and III models. In the class II model, the median (IQR) linear accuracies for #45, #34, and #37 were 0.33% (0.15%) 0.09% (0.09%), and 0.13% (0.15%), respectively. The linear accuracy at #45 was significantly higher than those at #34 ($P = 0.002$) and #37 ($P = 0.022$). In the class III model, the median (IQR) linear accuracies at #47 and #37 were 0.35% (0.08%) and 0.13% (0.18%), respectively. Linear accuracy at #47 was significantly higher than that at #37 ($P = 0.007$).

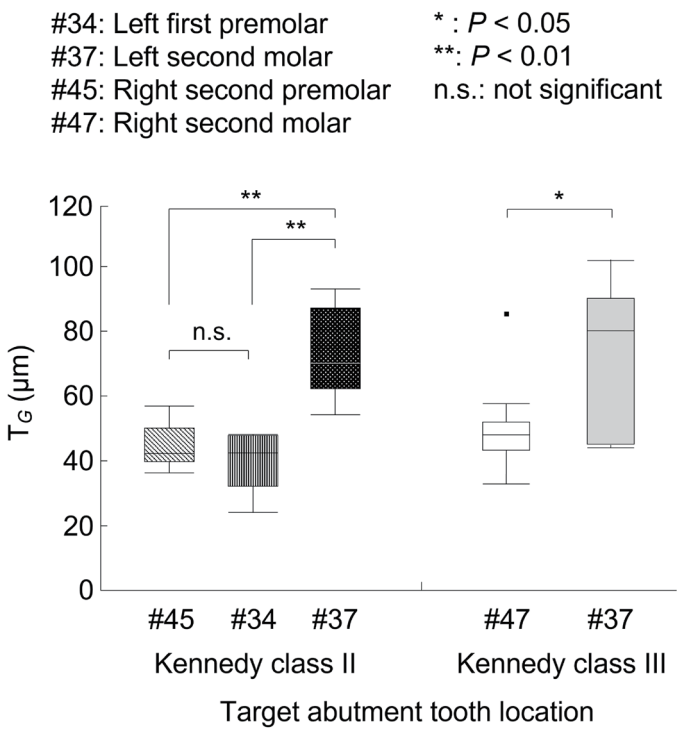

Fig. 4. Box plots of general trueness based on entire model superimposition (T_G) with comparisons between target teeth

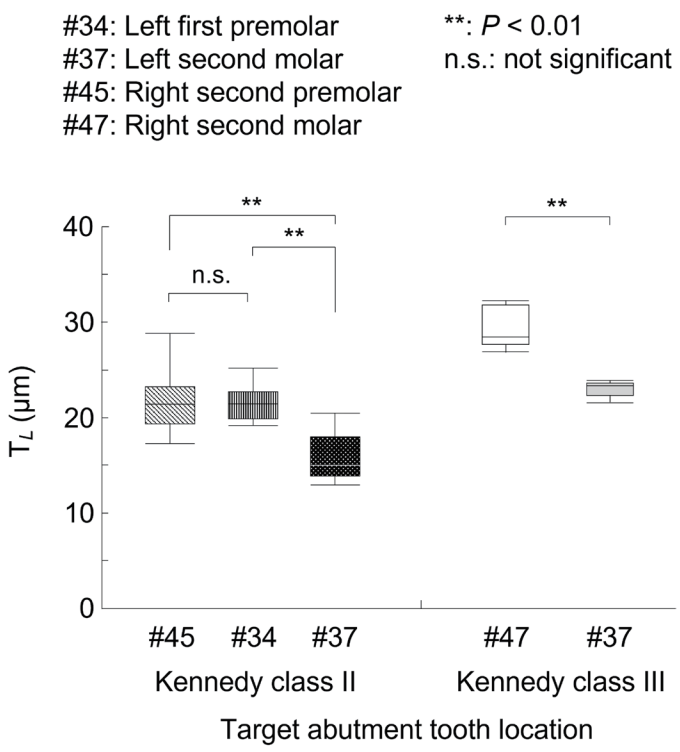

Fig. 5. Box plots of local trueness based on individual abutment tooth superimposition (T_L) with comparisons between target teeth

Table 1. Medians (IQR) coordinate deviation (μm) (deviation of the central coordinate of the sphere on each abutment tooth between reference data and IOS data based on the central coordinate of the sphere on the lingual frenum as the origin)

Reference model	Abutment tooth	Coordinate deviation (μm)					
		x-axis		y-axis		z-axis	
			$ $$		$ $$		$ $$
Class II	#34	-50.9 (28.0)	a -	8.1 (37.8)	a -	86.8 (50.3)	a -
	#37	-21.6 (99.0)	a -	-79.4 (66.3)	b -	41.9 (42.1)	a -
	#45	-102.1 (31.1)	b a	-26.5 (50.2)	b a	29.6 (51.3)	a a
	P value†	0.001*		<0.001*		0.082	
Class III	#37	-38.6 (45.4)	- -	-27.1 (29.4)	- -	63.9 (57.4)	- -
	#47	-138.6 (41.7)	- a	9.5 (46.2)	- b	95.4 (51.6)	- b
	P value‡	0.005*		0.047*		0.241	

IQR: interquartile range; #34: left first premolar; #37: left second molar; #45: right second premolar; and #47: right second molar. †: Friedman test. ‡: Wilcoxon signed-rank test. $: Same superscripted letters indicate groups not statistically significantly different with multiple comparisons in the class II model. $$: Same superscripted letters indicate groups not statistically significantly different with the Mann-Whitney U test between #45 in the class II model and #47 in the class III model. -: not applicable. *: $P<0.05$ is significant.

3.4. Comparison between the most posteriorly located abutment teeth

Figure 8 shows the comparison of T_G, T_L, and the linear accuracy between the most posteriorly located teeth in both models (#45 in the class II model and #47 in the class III model). T_L at #45 in the class II model was significantly lower than that at #47 in the class III model ($P < 0.001$), with no significant difference in T_G ($P = 0.190$) and linear accuracy ($P = 0.631$). Because all the rates of deviation in the distance between the lingual frenum and each target abutment tooth had positive values (> 0), the linear accuracy (absolute value of the rate of deviation) and rate of deviation were entirely the same.

The coordinate deviations of both the target teeth are listed in **Table 1**. The coordinate deviation at #45 in the class II model was significantly lower along the y-axis ($P = 0.035$) and z-axis ($P = 0.011$) than that along these axes at #47 in the class III model, with no significant difference in the x-axis coordinate deviation ($P = 0.052$).

4. Discussion

In this study, the accuracy of individual RPD abutment teeth in digital data obtained using an IOS was evaluated based on the reference data obtained using a high-accuracy desktop scanner. Tooth #37 in the Kennedy class II model had the following locational characteristics: 1) the most posterior location and 2) isolation from other teeth by the surrounding mucosal area. Because examination of the class II model could not clearly show how the locational characteristics of #37 affected the accuracy of the impression, the anteroposterior location of the target teeth was standardized by selecting the same teeth (#37 and #47) for the class III model, so that the comparison could focus on the effect of isolation of a tooth by mucosal area. In addition, to focus on the effect of the anteroposterior location of the tooth, the most posterior teeth, #45 in the class II model and #47 in the class III model, were compared. Overall, the results revealed that the abutment tooth location significantly affected the accuracy of the digital impression data for RPDs.

In this study, several measures were evaluated for representative data accuracy. First, we evaluated the general trueness of the abutment tooth area in the IOS data based on the entire model su-

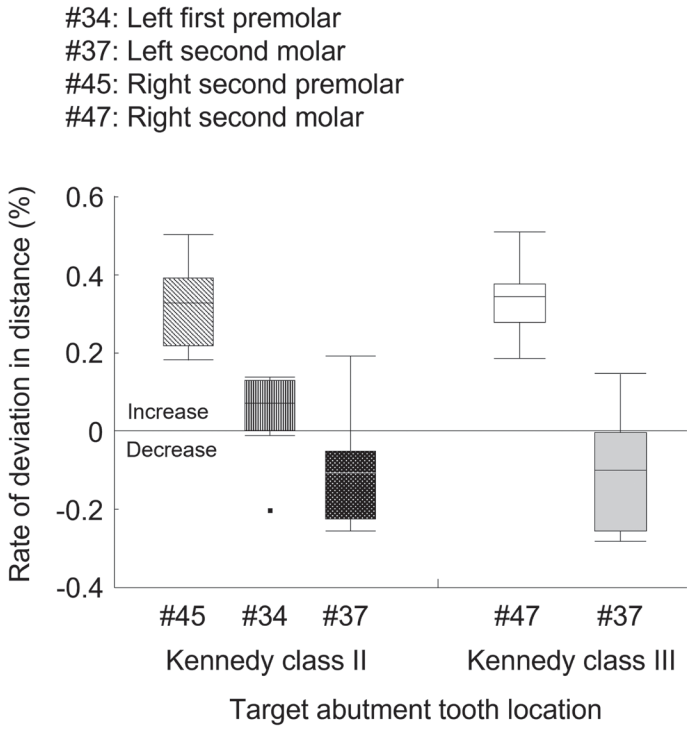

Fig. 6. Box plots of the rate of deviation in the distance from the lingual frenum (LF)

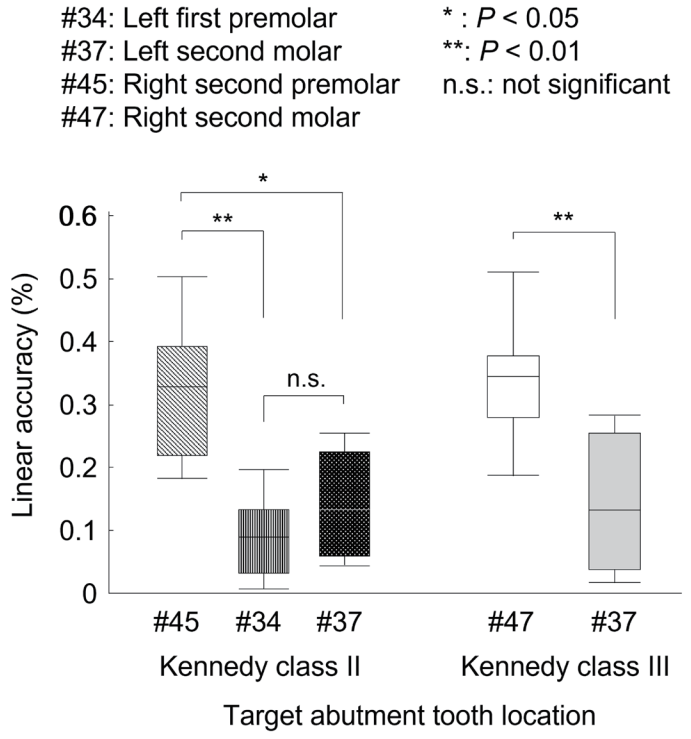

Fig. 7. Box plots of linear accuracy (the absolute value of the rate of deviation in the distance from the lingual frenum [LF]) with comparison between target teeth

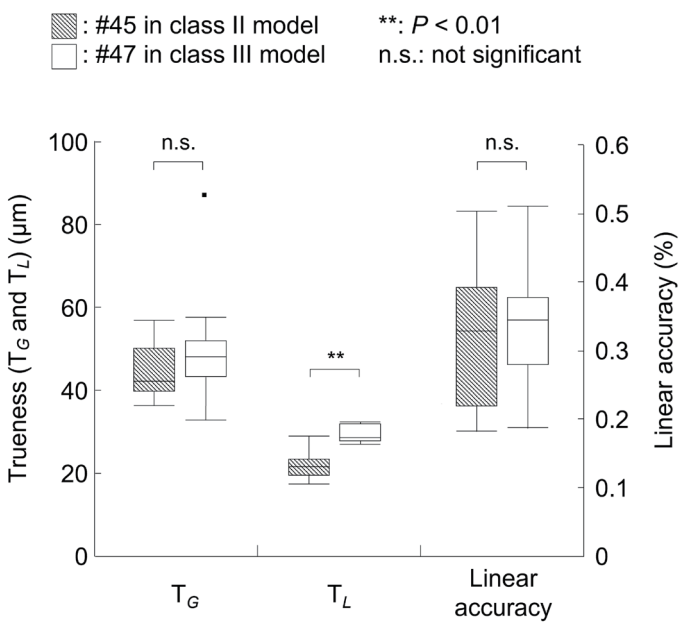

Fig. 8. Box plots of T_G, T_L, and linear accuracy with a comparison between #45 of the class II model and #47 of the class III model

perimposition (T_G), and local trueness based on individual abutment tooth superimposition (T_L). Because of the use of the best-fit method for data superimposition, the meaning of T_G differed from that of T_L. T_G indicated data distortion at the abutment tooth area in the IOS data, based on both displacement and geometric deformation of the entire dental arch. T_L indicated local data distortion, mainly involving geometric deformation.

When performing intra-model comparisons of T_G in both Kennedy class II and III models, the most inferior (highest) value was found at #37 (**Fig. 4**). However, in the inter-model T_G comparison between the most posterior teeth, there was no significant difference in T_G at #45 in the class II model and that at #47 in the class III model (**Fig. 8**). These findings indicate that the isolation of an abutment tooth surrounded by mucosa critically affects T_G, whereas the anteroposterior location does not. According to a previous study, a long-span mucosal area between two objects deteriorates the data trueness[13]. Moreover, the inferior trueness around mucosal areas purportedly results from a lack of landmarks for data stitching[14], and scanning with the placement of artificial landmarks on the mucosal area[15] followed by re-scanning after removing the landmarks[16] could improve data trueness.

Conversely, in intra-model comparisons of T_L, the most superior (lowest) value was identified at the most posterior abutment tooth (#37) in both models (**Fig. 5**). Additionally, in the inter-model comparison of T_L at the most posterior teeth, #45 in the class II model showed superior T_L compared to that at #47 in the class III model (**Fig. 8**). A previous study reported that data trueness calculated by data superimposition is influenced by the superimposition methods used[17]. In the present study, the T_L was inferior for teeth located furthest from the scanning origin. Consistent with our findings, Nagy et al. also observed inferior data deviation as the distance from the scanning origin increased, which was attributed to extensive data stitching[18].

Second, we evaluated the center coordinates of the spherules on the target abutment teeth, and the deviations in the coordinates (coordinate accuracy) and distance (linear accuracy) were calculated based on the lingual frenum as the reference point. Regarding coordinate accuracy, all the target abutment teeth were displaced to the right on the x-axis, close to the lingual frenum on the y-axis (except for the second molar in the class III model), and upward along the z-axis (**Table 1**). Additionally, a greater span between the abutment tooth and the scanning origin correlated with a greater displacement of the coordinate along the x-axis. These findings are consistent with those of a previous study[17]. However, a more posterior location of the target tooth also reportedly indicates its greater displacement in the buccal direction based on color map images with RMS values[19]. The displacement of the coordinate is affected not only by the tooth displacement but also by its three-dimensional deformation. In this study, the color map revealed various colors depending on the area within a single tooth crown (**Fig. 2C**), suggesting that the displacement of the coordinate partially depends on spherule location.

Considering the linear accuracy, the tooth located furthest from the scanning origin showed the most inferior linear accuracy in both models (**Fig. 7**). Similar to the T_L and x-coordinate of the spherule center, the linear accuracy of the abutment tooth was affected by its distance from the scanning origin. However, the present study focused on the anteroposterior location of the abutment tooth and the effect of its isolation in the oral cavity. Our study protocol could not independently clarify the effects of these locational conditions and the distance from the scanning origin. However, only #37, which was isolated from the remaining teeth by the mucosal area, showed a negative rate of deviation, indicating that the distance from the lingual frenum decreased in the impressions of both models (**Fig. 6**). This finding suggests that the mucosal area causes a decrease in the distance between two points on the digital impression.

This study revealed that the accuracy of digital impressions obtained using an IOS for RPDs can be affected by the anteroposterior location of the abutment tooth, whether it is isolated with no adjacent teeth or surrounded by mucosa, and its distance from the scanning origin. Conversely, the median T_G, T_L, and coordinate deviation were less than 81.0 µm, 28.7 µm, and -138.6 µm, respectively. The trueness of a conventional impression of a partially edentulous dental arch taken using a custom tray and elastic silicone impression material has been reported to be 122-157 µm[6]. Furthermore, in this study, the linear accuracy was less than 0.4% for all target abutment teeth, which is within the clinically acceptable range set by the American Dental Association (ADA). The ADA accepts a range of 0.5% or less dimensional change at 24 h after recording an impression with conventional materials[20]. Therefore, the accuracy of digital impressions for RPDs may be equal or superior to that of conventional impressions, suggesting that digital impressions using an IOS have a clinically acceptable accuracy.

This study had several limitations. First, it was a simulation experiment using dental models that could not completely reproduce an oral environment containing saliva. Additionally, we did not use scanned powders to eliminate the effects of the thickness of the powder layer. Scanning without scanning powders may affect the accuracy of the digital data. Second, we used only one IOS. However, the type of IOS used can reportedly affect data accuracy[21]. Therefore, it remains unclear whether our findings can be extrapolated to digital impressions obtained using other types of IOS. Third, we analyzed the data accuracy only for individual RPD abutment tooth regions. Further studies are required to verify the data accuracy of digital impressions, including those of the mucosal area and residual teeth other than the abutment teeth.

5. Conclusions

Within the limitations of this study, our findings suggest that when an RPD abutment tooth is isolated with no adjacent teeth and is surrounded by mucosa, there is a risk of data distortion of the abutment tooth relative to the entire dental arch and mesial displacement of the tooth in the digital impression obtained using an IOS. Additionally, a greater distance between the RPD abutment tooth and the scanning origin can cause local data distortion of the RPD abutment tooth and reduce linear accuracy, whereas the anteroposterior location of the RPD abutment teeth does not critically affect the accuracy of the data. These results also indicate that the accuracy of the digital impressions obtained using an IOS is acceptable for clinical applications.

Acknowledgments

This study was funded by grants (Nos. 17K11741 and 19K19086) from the Japan Society for Promotion of Science.

Conflicts of interest

The authors declare no conflict of interest.

References

[1] Stapleton BM, Lin WS, Ntounis A, Harris BT, Morton D. Application of digital diagnostic impression, virtual planning, and computer-guided implant surgery for a CAD/CAM-fabricated, implant-supported fixed dental prosthesis: A clinical report. J Prosthet Dent. 2014;112:402–8. https://doi.org/10.1016/j.prosdent.2014.03.019, PMID:24831749

[2] Rayyan MM, Aboushelib M, Sayed NM, Ibrahim A, Jimbo R. Comparison of interim restorations fabricated by CAD/CAM with those fabricated manually. J Prosthet Dent. 2015;114:414–9. https://doi.org/10.1016/j.prosdent.2015.03.007, PMID:26001490

[3] Fang JH, An X, Jeong SM, Choi BH. Development of complete dentures based on digital intraoral impressions—case report. J Prosthodont Res. 2018;62:116–20. https://doi.org/10.1016/j.jpor.2017.05.005, PMID:28625663

[4] Carneiro Pereira AL, Martins de Aquino LM, Carvalho Porto de Freitas RF, Soares Paiva Tôrres AC, da Fonte Porto Carreiro A. CAD/CAM-fabricated removable partial dentures: a case report. Int J Comput Dent. 2019;22:371–9. PMID:31840145

[5] Nishiyama H, Taniguchi A, Tanaka S, Baba K. Novel fully digital workflow for removable partial denture fabrication. J Prosthodont Res. 2020;64:98–103. https://doi.org/10.1016/j.jpor.2019.05.002, PMID:31229550

[6] Hayama H, Fueki K, Wadachi J, Wakabayashi N. Trueness and precision of digital impressions obtained using an intraoral scanner with different head size in the partially edentulous mandible. J Prosthodont Res. 2018;62:347–52. https://doi.org/10.1016/j.jpor.2018.01.003, PMID:29502933

[7] Tasaka A, Uekubo Y, Mitsui T, Kasahara T, Takanashi T, Homma S, *et al.* Applying intraoral scanner to residual ridge in edentulous regions: in vitro evaluation of inter-operator validity to confirm trueness. BMC Oral Health. 2019;19:264. https://doi.org/10.1186/s12903-019-0918-y, PMID:31791324

[8] International Organization for Standardization. Accuracy (trueness and precision) of measurement methods and results. Part 1: General principles and definitions. 1994, https://www.iso.org/standard/69418.html, [accessed 16 May 2022].

[9] Lee JH, Yun JH, Han JS, Yeo ISL, Yoon HI. Repeatability of intraoral scanners for complete arch scan of partially edentulous dentitions: an in vitro study. J Clin Med. 2019;8:1187. https://doi.org/10.3390/jcm8081187, PMID:31398851

[10] Dold P, Bone MC, Flohr M, Preuss R, Joyce TJ, Deehan D, *et al.* Validation of an optical system to measure acetabular shell deformation in cadavers. Proc Inst Mech Eng H. 2014;228:781–6. https://doi.org/10.1177/0954411914546562, PMID:25085696

[11] Oh KC, Park JM, Moon HS. Effects of scanning strategy and scanner type on the accuracy of intraoral scans: A new approach for assessing the accuracy of scanned data. J Prosthodont. 2020;29:518–23. https://doi.org/10.1111/jopr.13158, PMID:32133690

[12] Luthardt RG, Koch R, Rudolph H, Walter MH. Qualitative computer aided evaluation of dental impressions in vivo. Dent Mater. 2006;22:69–76. https://doi.org/10.1016/j.dental.2005.02.015, PMID:16040117

[13] Flügge T, Att W, Metzger M, Nelson K. Precision of dental implant digitization using intraoral scanners. Int J Prosthodont. 2016;29:277–83. https://doi.org/10.11607/ijp.4417, PMID:27148990

[14] Andriessen FS, Rijkens DR, van der Meer WJ, Wismeijer DW. Applicability and accuracy of an intraoral scanner for scanning multiple implants in edentulous mandibles: A pilot study. J Prosthet Dent. 2014;111:186–94. https://doi.org/10.1016/j.prosdent.2013.07.010, PMID:24210732

[15] Kim JE, Amelya A, Shin Y, Shim JS. Accuracy of intraoral digital impressions using an artificial landmark. J Prosthet Dent. 2017;117:755–61. https://doi.org/10.1016/j.prosdent.2016.09.016, PMID:27863856

[16] Shimizu T, Tasaka A, Wadachi J, Yamashita S. A new proposal for improving the accuracy of intraoral scanning for partially edentulous residual ridge. J Prosthodont Res. Online ahead of print. https://pubmed.ncbi.nlm.nih.gov/36031353/

[17] Vág J, Nagy Z, Simon B, Mikolicz Á, Kövér E, Mennito A, *et al.* A novel method for complex three-dimensional evaluation of intraoral scanner accuracy. Int J Comput Dent. 2019;22:239–49. https://pubmed.ncbi.nlm.nih.gov/31463488/ PMID:31463488

[18] Nagy Z, Simon B, Mennito A, Evans Z, Renne W, Vág J. Comparing the trueness of seven intraoral scanners and a physical impression on dentate human maxilla by a novel method. BMC Oral Health. 2020;20:97. https://doi.org/10.1186/s12903-020-01090-x, PMID:32264943

[19] Patzelt SBM, Emmanouilidi A, Stampf S, Strub JR, Att W. Accuracy of full-arch scans using intraoral scanners. Clin Oral Investig. 2014;18:1687–94. https://doi.org/10.1007/s00784-013-1132-y, PMID:24240949

[20] Marcinak CF, Draughn RA. Linear dimensional changes in addition curing silicone impression materials. J Prosthet Dent. 1982;47:411–3. https://doi.org/10.1016/S0022-3913(82)80092-9, PMID:6951042

[21] Kim RJY, Park JM, Shim JS. Accuracy of 9 intraoral scanners for complete-arch image acquisition: A qualitative and quantitative evaluation. J Prosthet Dent. 2018;120:895–903.e1. https://doi.org/10.1016/j.prosdent.2018.01.035, PMID:30006228